Supporting Information:

Graphene Quantum Dots: Efficient Mechanosynthesis, White-Light and Broad Linearly Excitation-Dependent Photoluminescence and Growth Inhibition on Bladder Cancer Cells

Maojun Deng, Xiaocong Cao, Lifang Guo, Hui Cao, Zhongliang Wen, Chaochao Mao, Kaimin Zuo, Xin Chen,* Xiaolong Yu,* Wenbing Yuan*

Table S1. Experimental conditions of mechanochemical synthesis of N-GQD

Samples	Instrument types	Graphite amount	Melamine amount	KOH amount	Grinding frequency (rpm)	Yield (%)
N-GQDs-300	QM-3SP04	20mg	60mg	300mg	300	33.7
N-GQDs-600	QM-3SP04	20mg	60mg	300mg	600	61.1
N-GQDs-500-0.5	QM-3SP2	0.5g	1.5g	7.5g	500	26.3
N-GQDs-500-1.0	QM-3SP2	1.0g	3.0g	15.0g	500	23.8
N-GQDs-500-1.5	QM-3SP2	1.5g	4.5g	22.5g	500	20.4
N-GQDs-500-2.0	QM-3SP2	2.0g	6.0g	30.0g	500	18.9

Table S2. Carbon, nitrogen and oxygen bonding composition, (N1s)/(C1s) and (O1s)/(C1s) atomic ratios determined from the full-range XPS spectra (Figures 1k, 2h, S3 and S15a) for N-GQDs.

Samples	C%	N%	O%	N1s/C1s	O1s/C1s
N-GQDs-300	55.75	8.95	35.30	0.16	0.63
N-GQDs-600	56.71	11.08	32.21	0.20	0.57
N-GQDs-500-0.5	55.42	14.18	30.40	0.26	0.55
N-GQDs-500-1.0	52.58	11.77	35.65	0.22	0.68
N-GQDs-500-1.5	56.46	10.26	33.28	0.18	0.59
N-GQDs-500-2.0	60.75	7.09	32.16	0.12	0.53

Table S3. Carbon bonding composition determined from the C1s XPS (Figures 1l, 2i, S4, S15b) for N-GQDs.

Sample name	Carbon Bonding Composition (%)				
	C-C/C-H	C-N	C-O	C=O	O-C=O
N-GQDs-300	49	4	20	24	3
N-GQDs-600	53	5	19	20	3
N-GQDs-500-0.5	49	6	19	23	3
N-GQDs-500-1.0	45	5	23	20	6

N-GQDs-500-1.5	51	4	21	19	4
N-GQDs-500-2.0	53	6	24	13	5

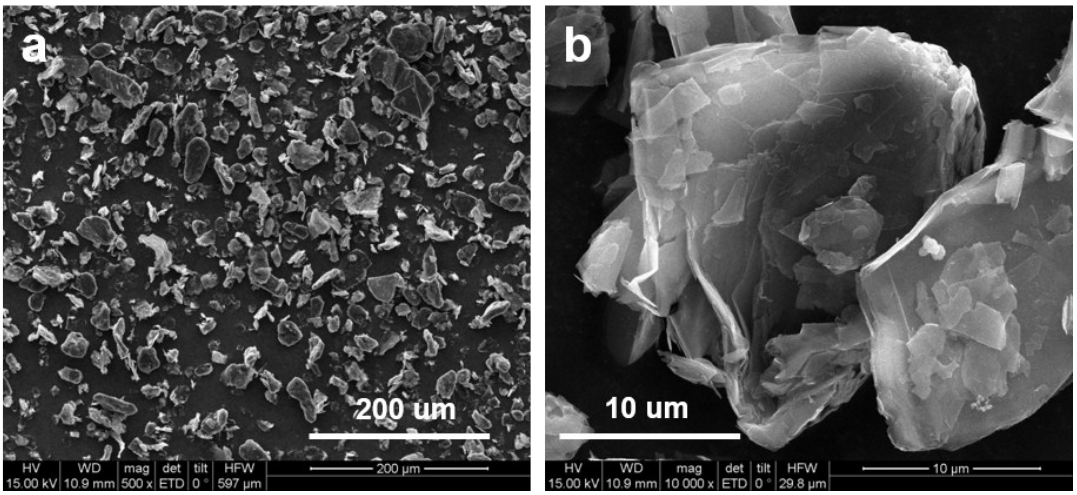

Figure S1. SEM images of the pristine graphite, which was used as a starting material to prepare N-GQDs.

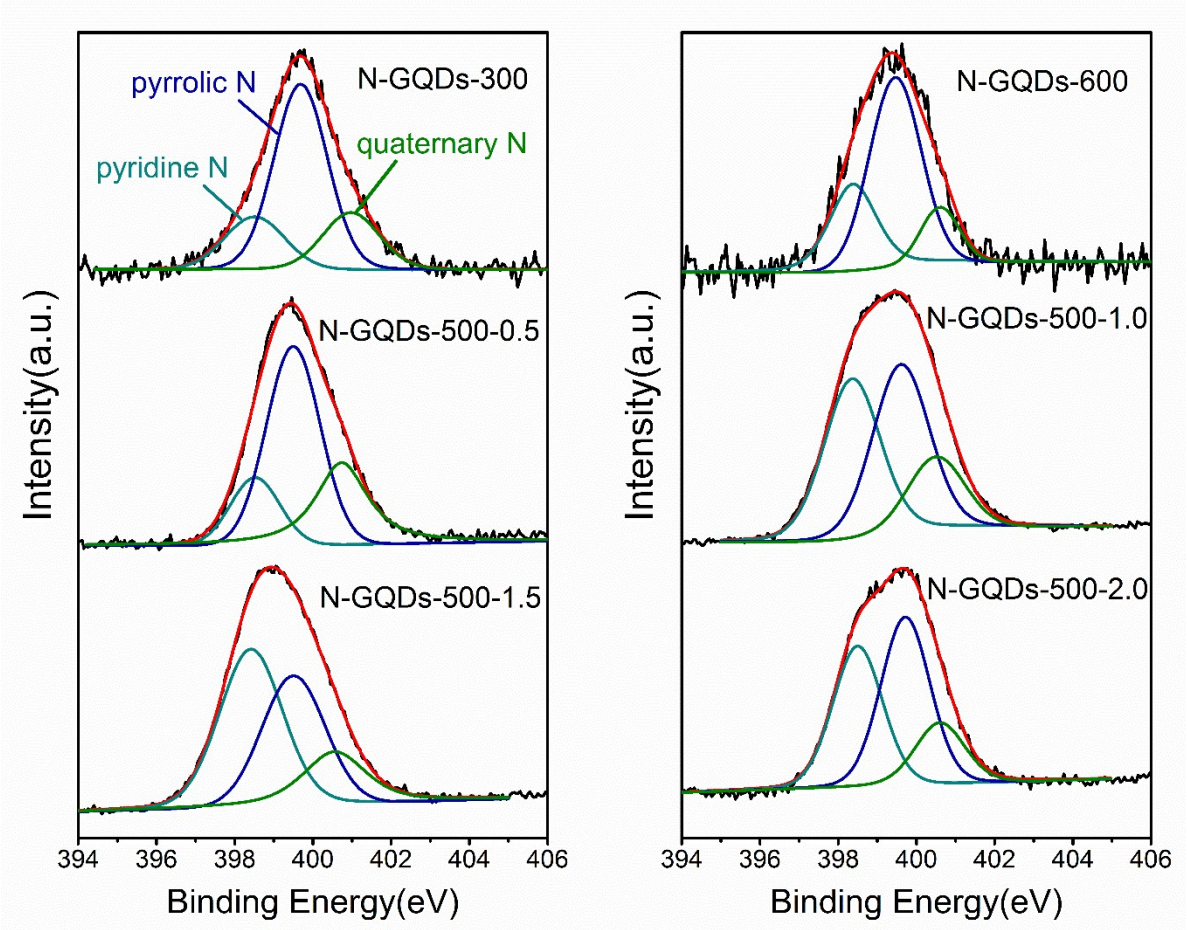

Figure S2. High-resolution XPS N1s spectra for samples N-GQDs-300, N-GQDs-600, N-GQDs-500-0.5, N-GQDs-500-1.0, N-GQDs-500-1.5 and N-GQDs-500-2.0.

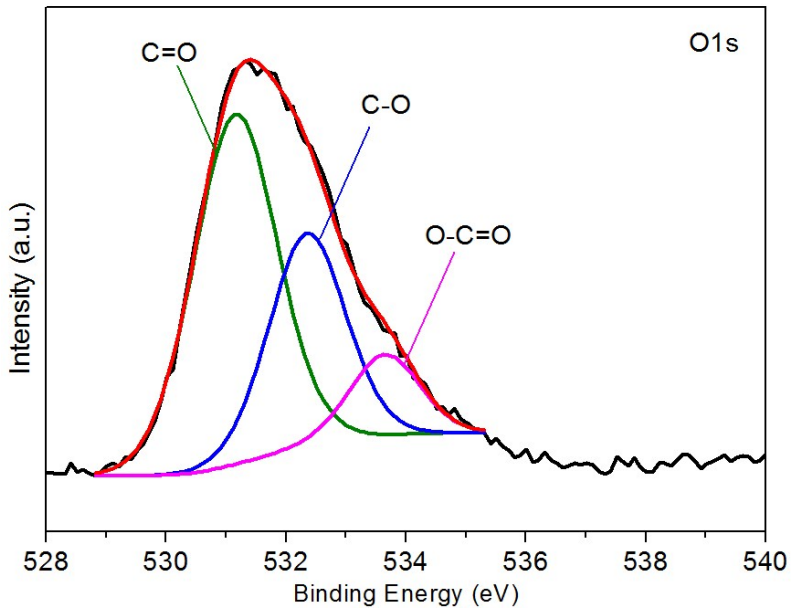

Figure S3. High resolution O1s XPS spectrum of N-GQDs-300.

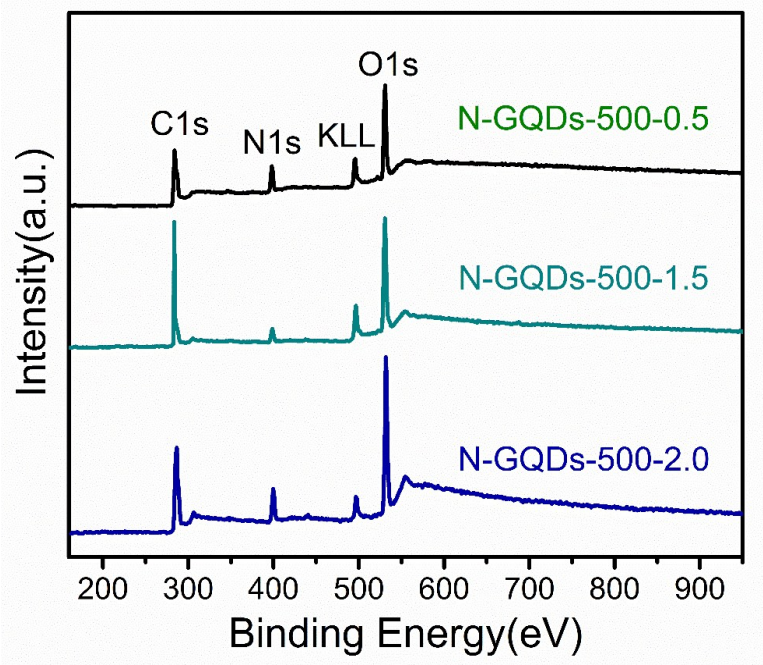

Figure S4. Survey XPS spectra for large-scale synthesized samples N-GQDs-500-0.5, N-GQDs-500-1.5 and N-GQDs-500-2.0.

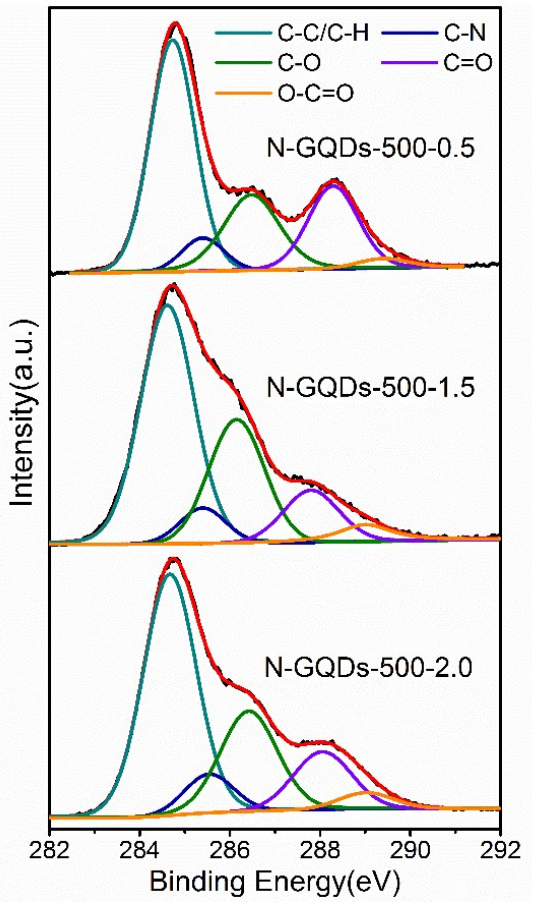

Figure S5. High-resolution C 1s spectra for samples N-GQDs-500-0.5, N-GQDs-500-1.5 and N-GQDs-500-2.0.

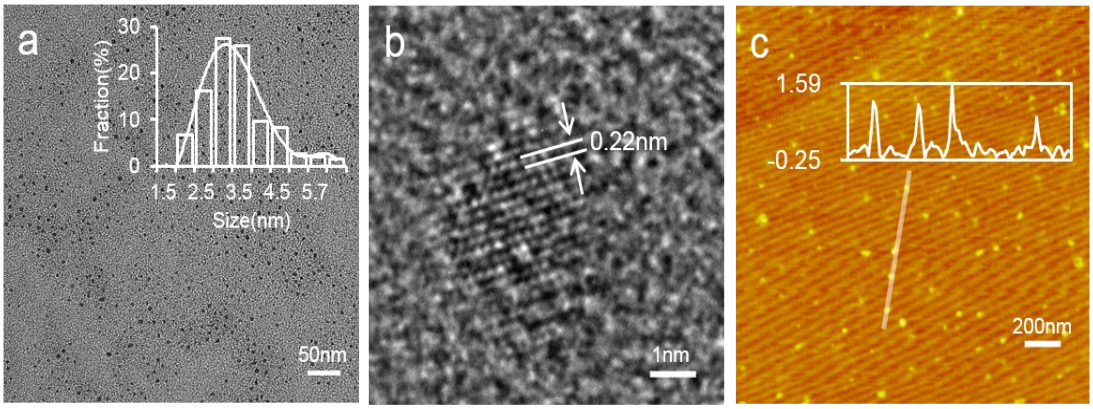

Figure S6. (a-c) TEM, HRTEM and AFM images of large-scale synthesized sample N-GQDs-500-2.0. The inset of (b) and (c) are size distribution of the dots and height profile of the selected area respectively.

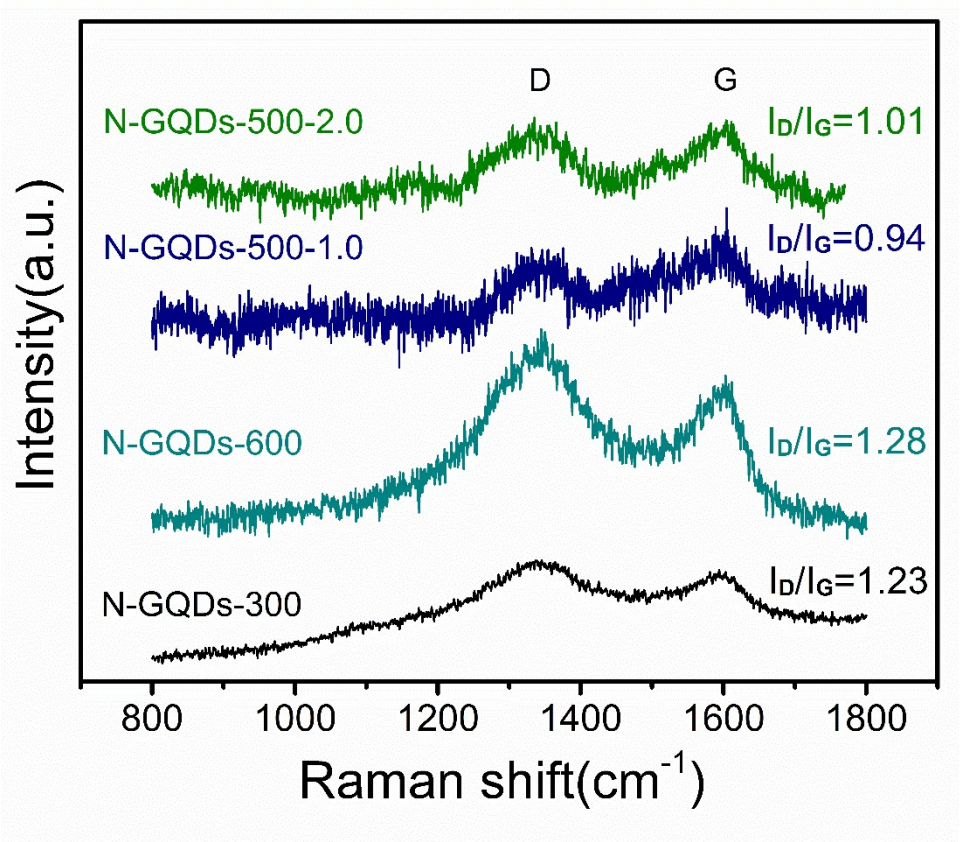

Figure S7. Raman spectra of N-GQDs-300, N-GQDs-600, N-GQDs-500-1.0 and N-GQDs-500-2.0 respectively.

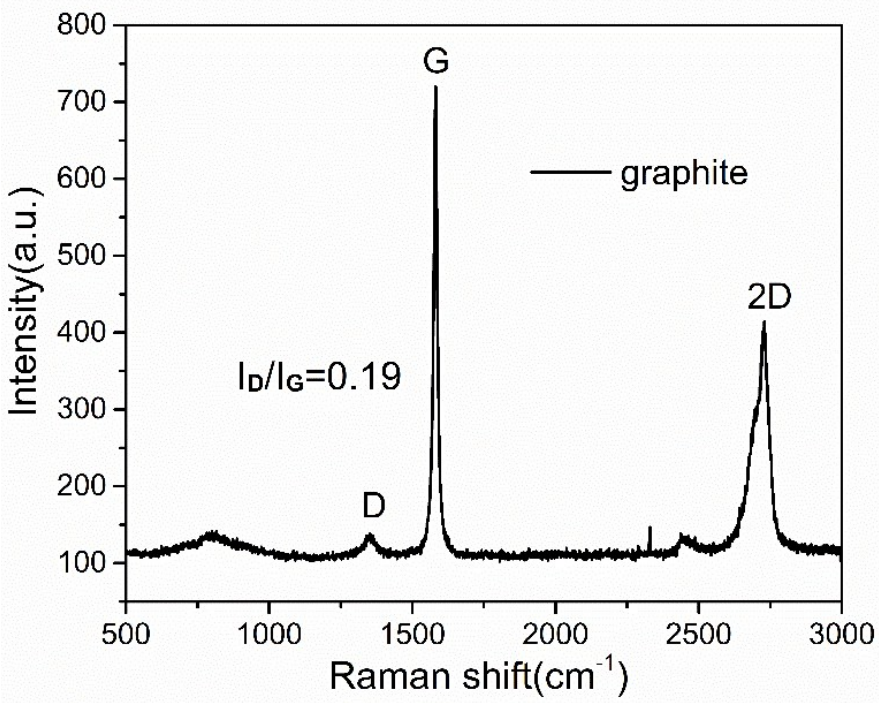

Figure S8. Raman spectrum of the pristine graphite, which was used as a starting material to prepare N-GQDs.

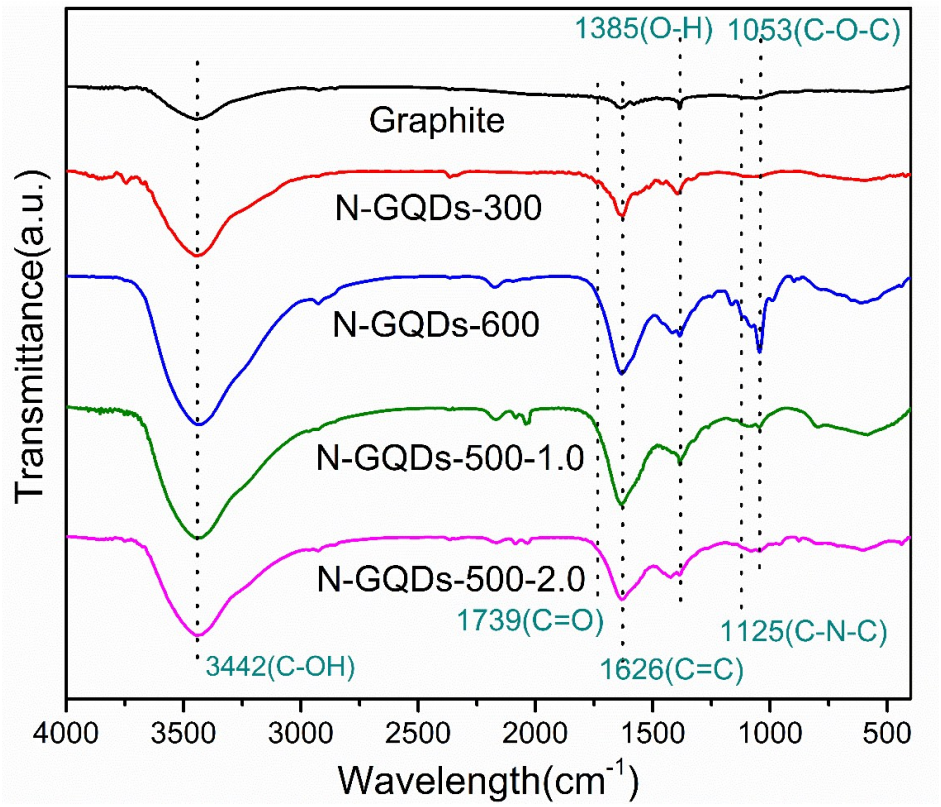

Figure S9. FT-IR spectra of samples graphite, N-GQDs-300, N-GQDs-600, N-GQDs-500-1.0 and N-GQDs-500-2.0.

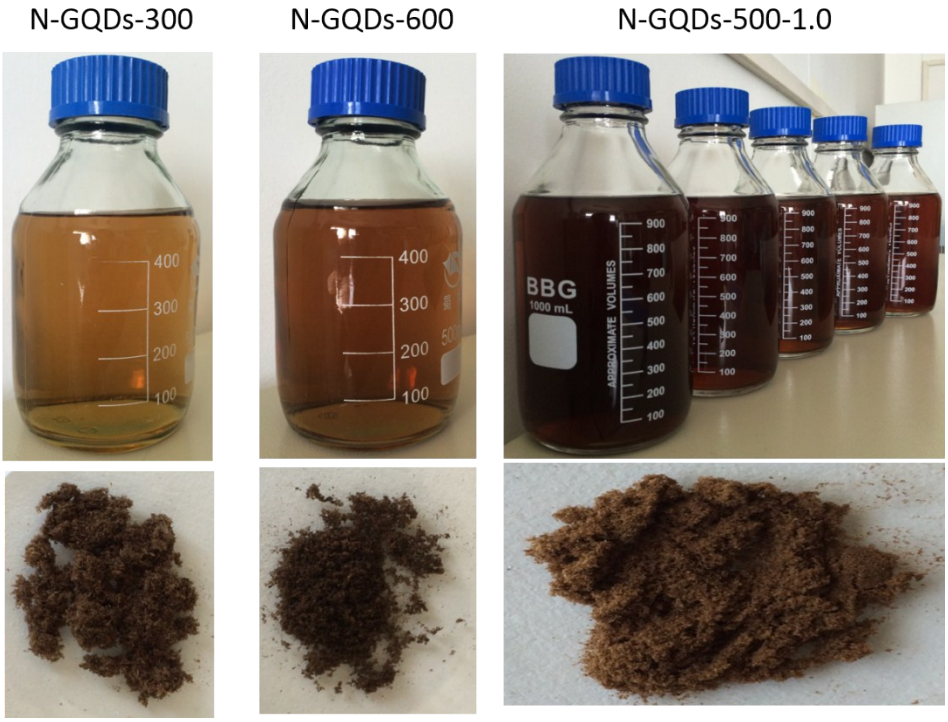

Figure S10. Photographs of the as-obtained N-GQDs-300, N-GQDs-600 and N-GQDs-500-1.0 in solid powder and aqueous solution state.

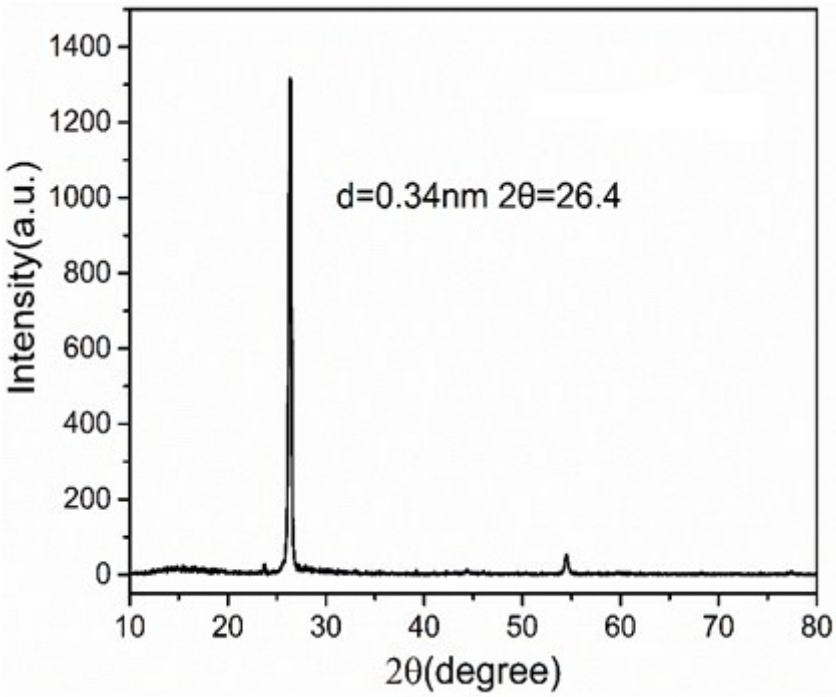

Figure S11. PXRD pattern of the pristine graphite, which was used as a starting material to prepare N-GQDs.

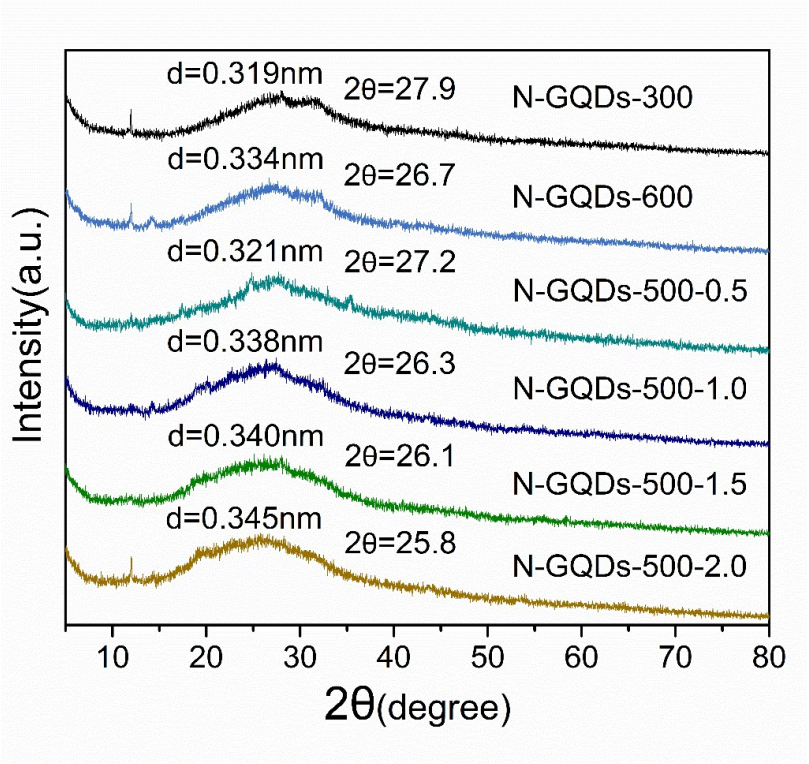

Figure S12. PXRD patterns of N-GQDs-300, N-GQDs-600, N-GQDs-500-0.5, N-GQDs-500-1.0, N-GQDs-500-1.5, and N-GQDs-500-2.0.

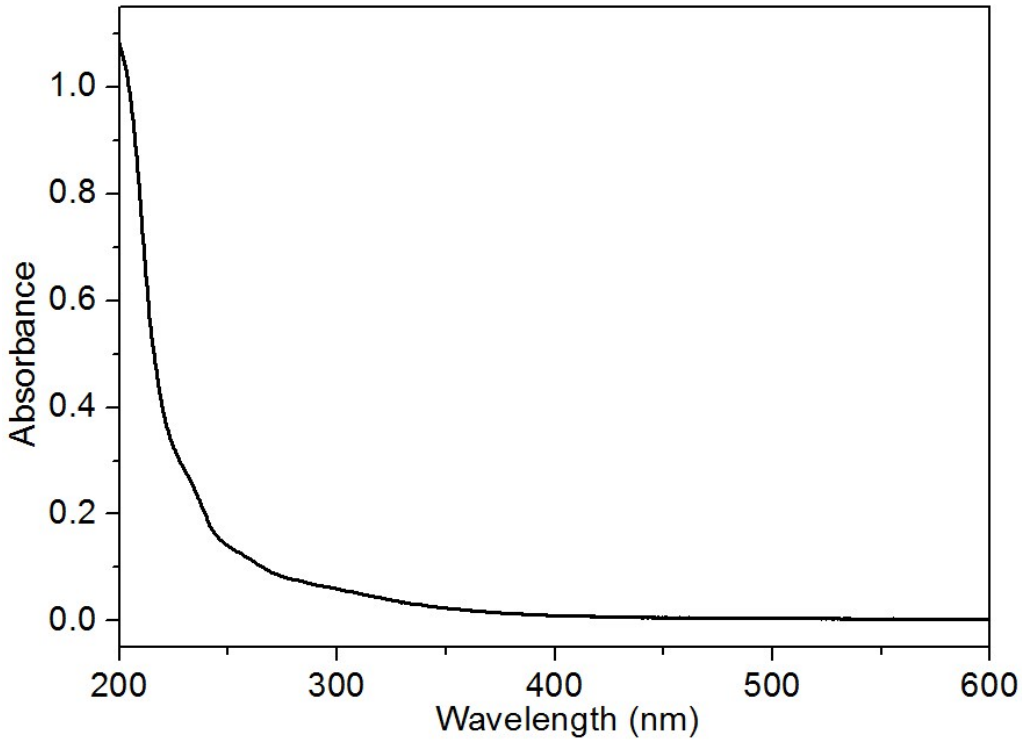

Figure S13. UV-Vis spectrum of N-GQDs-300 aqueous solution

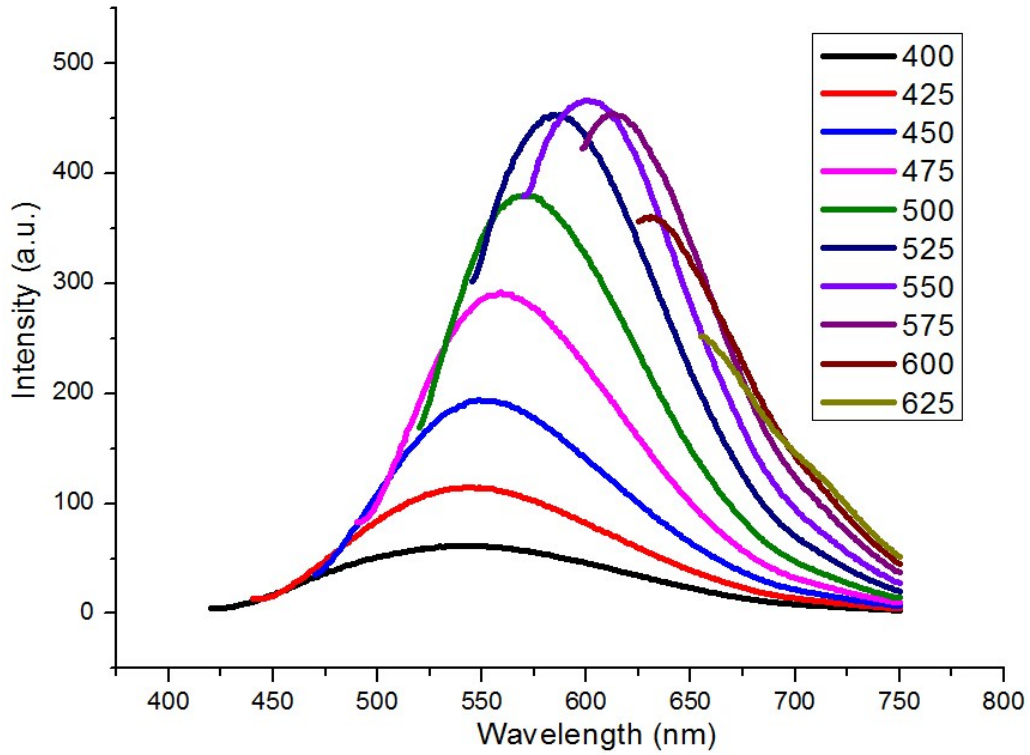

Figure S14. PL spectra of N-GQDs-600 aqueous solution depended on different excitation.

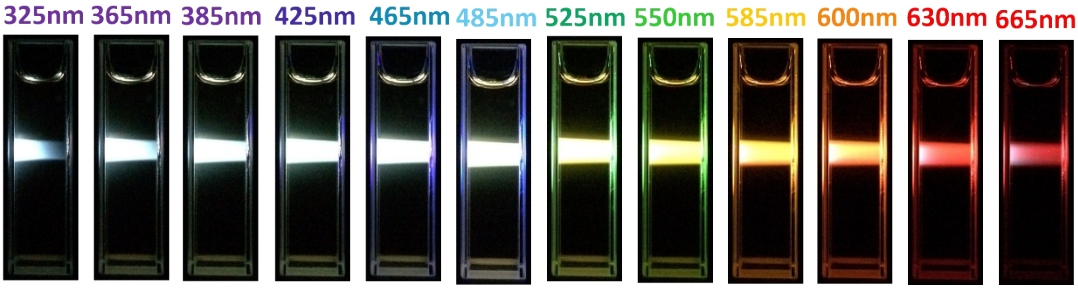

Figure S15. Optical photographs of N-GQDs-600 aqueous solution depended on different excitation wavelengths from 325-665nm.

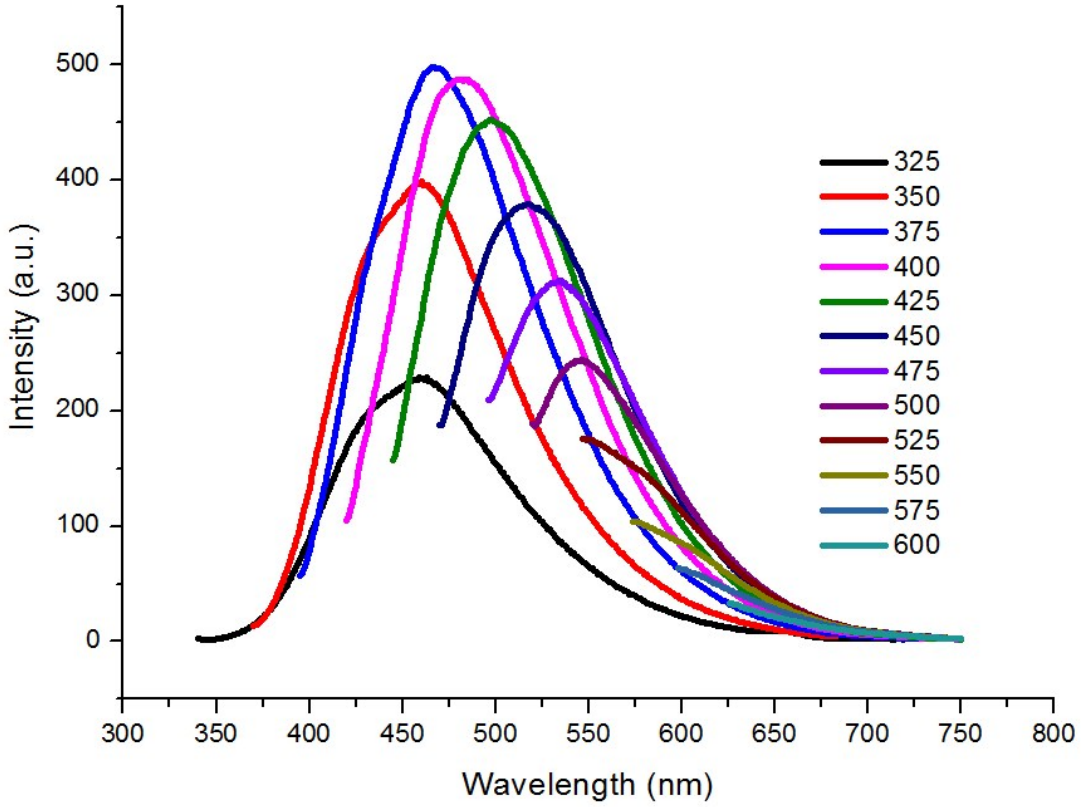

Figure S16. PL spectra of N-GQDs-500-1.0 aqueous solution depended on different excitation.

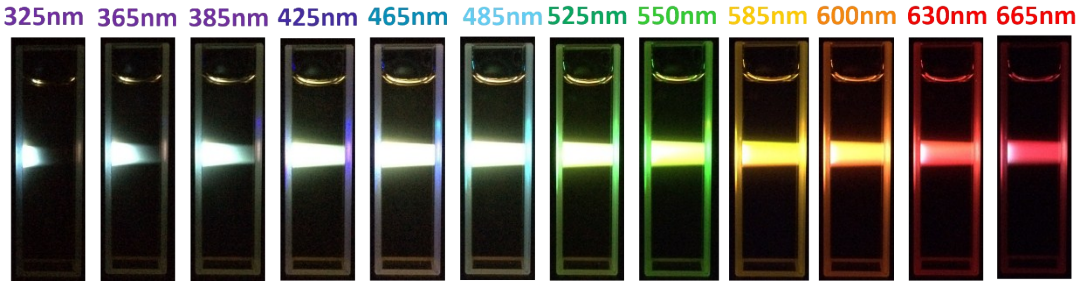

Figure S17. Optical photographs of N-GQDs-500-1.0 aqueous solution depended on excitation wavelengths from 325-665nm.

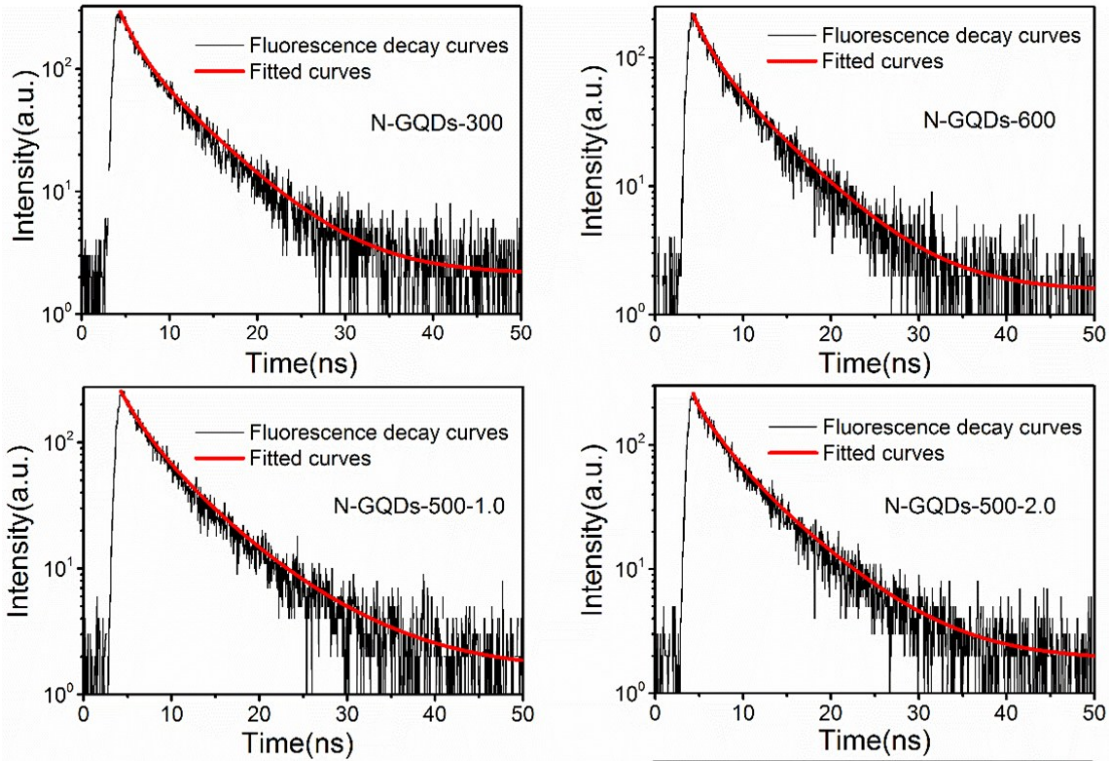

Figure S18. PL lifetime of N-GQDs aqueous solution excited at 468 nm.